RSC Advances

ROYAL SOCIETY OF CHEMISTRY

www.rsc.org/advances

RSC Advances

RSCPublishing

ARTICLE

Photocatalysis induces bioactivity of an organic polymer based material

Cite this: DOI: 10.1039/x0xx00000x

Yanling Cai,[a]* Maria Strømme,[a] Peng Zhang,[a] Håkan Engqvist[b] and Ken Welch [a]*

Received 00th January 2012,
Accepted 00th January 2012

DOI: 10.1039/x0xx00000x

www.rsc.org/

Several materials, like bioglasses, sintered hydroxyapatite and Ti metals and alloys, have the ability to bond to living bone *in vivo*, which is a desirable property of biomaterials called bioactivity. In this work, we present a novel strategy to develop bioactivity on the non-bioactive surface of a resin-TiO_2 nanocomposite through photocatalysis. The results show that UV irradiation (365 nm, 10 mW/cm^2) for 8 to 16 h on the resin-TiO_2 nanocomposite immersed in water induces bioactivity as indicated by hydroxyapatite growth following immersion of the samples in Dulbecco's phosphate buffered saline for 7 days at 37 °C. While a non-irradiated resin-TiO_2 surface did not show any hydroxyapatite deposition, a surface with 16 h of UV irradiation was fully covered by hydroxyapatite. *In vitro* cell adhesion of osteoblast-like MG63 cells confirmed the biocompatibility and bioactivity of the resin-TiO_2 surfaces with a hydroxyapatite deposition layer, while the non-irradiated resin-TiO_2 surface showed no cell adhesion. Resin-TiO_2 nanocomposites, with or without UV irradiation, were proved to be nontoxic to two human cell lines, human dermal fibroblasts (hDF) and MG63 cells. It was also shown that an increasing dose of UV irradiation decreased bacterial adhesion, which is an additional benefit of the UV treatment and a favourable property for biomedical applications. The combined benefits of biocompatibility, bioactivity, decreased bacterial adhesion and the highly efficient disinfection property of TiO_2 photocatalysis under UV light make this resin-TiO_2 material an interesting candidate for implant and biomedical device applications.

Introduction

Since the discovery of spontaneous bonding between living bone and Bioglass® (Na_2O-CaO-SiO_2-P_2O_5) through a bone-like apatite layer in 1972 [1], bioactivity has become a sought-after property in biomaterial development [2, 3]. Many types of materials, like ceramics, (e.g. sintered hydroxyapatite, sintered β-tricalcium phosphate and wollastonite) [4]. Ti metals and alloys (e.g. Ti-6Al-4V, Ti-15Mo-5Zr-3Al and Ti-6Al-2Nb-Ta) [5] and the anatase and rutile [6, 7] phases of crystalline TiO_2 have been shown to be bioactive and widely used clinically as implant materials. Bioactivity can also be achieved on polymers (e.g. poly-methylmethacrylate, poly-ethylene terephthalate, Nylon 6, polyamide 6 and polyethylene) through the formation of apatite nuclei on their surfaces upon contact with granular particles of CaO-SiO_2-based glass in simulated body fluid (SBF) [5].

The *in vivo* bone-bonding ability of a material can be evaluated through an *in vitro* test, which is based on the degree of hydroxyapatite layer formation on the surface of the material when soaked in acellular body-like fluid with pH value and ion concentrations nearly equal to those of human blood plasma, e.g. SBF [4, 8] and Dulbecco's phosphate buffered saline (DPBS) [6, 9]. This method has been proven to be able to qualitatively and quantitatively predict *in vivo* bone-bonding bioactivity [10].

The mechanism of hydroxyapatite growth on the rutile phase of TiO_2 in SBF (pH 7.4) relies on the existence of Ti-OH on the rutile surface and the formation of Ti-O$^-$ groups due to the isoelectric point of rutile of about 5.9 [11, 12]. The negative Ti-O$^-$ groups attract Ca^{2+} ions in the SBF to form a slightly positively charged layer of calcium titanate, which then attracts PO_4^{3-} ions to form amorphous calcium phosphate. A layer of bone-like hydroxyapatite, which thermodynamically favours the crystalline form in the wet condition, is eventually formed on the surface of rutile TiO_2 material [13].

Recently, bioactivity in polymer-TiO_2 composites has been shown by Boccaccini et al. [14, 15] and in our former work [16]. However, in the study by Boccaccini et al., 21 days immersion in SBF was required for hydroxyapatite growth on poly-D, L-lactic acid (PDLLA) containing 20 wt% TiO_2 nanoparticles [14]. As well, in our former work with TiO_2 nanoparticles encased in a commercially available dental adhesive polymer, only a sparse coverage of small hydroxyapatite crystals was achieved [16]. Since it has been shown that the rate and degree of hydroxyapatite formation *in vitro* quantitatively predicts the *in vivo* bone-bonding performance

[10], it is desirable to achieve enhanced bioactivity with better hydroxyapatite coverage of material within shorter period of time.

In this work, we present a new strategy for developing bioactivity on a polymer-TiO_2 nanocomposite material through photocatalysis of TiO_2. For the first time, photocatalysis of TiO_2 is shown to induce bioactivity on an organic polymer material. The influence of photocatalysis on the surface roughness, hydrophobicity, morphology, as well as the biological properties, including hydroxyapatite formation, cytotoxicity, bacteria and cell adhesion, were investigated. Combined with the well-known highly efficient antibacterial property under UV light [16, 17], TiO_2 nanoparticle composite materials show promise for novel biomaterial applications.

Materials and Methods

Resin-TiO_2 nanocomposite

The resin material, with a composition primarily designed for dental materials [18], consists of two types of monomer, 2, 2-bis [4-(2-hydroxy-3- methacryloxypropoxy) phenyl-propane (BisGMA, Polysciences Europe GmbH, Eppelheim, Germany) and 2-hydroxyethyl methacrylate (HEMA, Sigma-Aldrich, Schnelldorf, Germany), in a 55/45 wt/wt ratio. Photoinitiator and coinitiators were added as follows: 0.5 mol% camphorquinone (CQ); 0.5 mol% 2-(dimethylamino) ethyl methacrylate (DMAEMA); 0.5 mol% ethyl-4-(dimethylamino) benzoate (EDMAB); and 1 wt% diphenyliodonium hexafluorophosphate (DPIHP) (all from Sigma-Aldrich, Steinheim, Germany).

The resin-TiO_2 nanocomposite was prepared by mixing 20 wt% of TiO_2 nanoparticles (P25, Evonik Industries (previously Degussa) AG, Germany) into the resin. The container with the resin-TiO_2 mixture was sonicated for 1 h in order to decrease TiO_2 nanoparticle aggregation. The mixture was then cast in Teflon molds (diameter 8 mm, thickness 1 mm) and 460 nm light (BlueLEX GT1200, Monitex, Taiwan) was applied on each sample for 30 s under N_2 flow to cure the resin. The resin-TiO_2 disks produced for this study were randomly grouped for all tests. Pure resin disks without TiO_2 (resin disks) were also produced for use in bioactivity, cytotoxicity and cell adhesion tests.

UV irradiation treatment

The resin-TiO_2 sample disks produced for this study were divided into three groups: resin-TiO_2 disks without UV irradiation treatment (Control disks); resin-TiO_2 disks treated with UV irradiation under ambient conditions (UV, disks in air) and resin-TiO_2 disks treated with UV irradiation while immersed in water (UV, disks in water).

To treat the resin-TiO_2 disks with UV irradiation in ambient conditions, the disks were placed in a well of a 6-well plate covered with a transparent lid and irradiated with a UV-A diode (peak wavelength at 365 nm, NSCU033B (T), Nichia, Japan) having an intensity of 10 mW/cm^2 (UV light meter, UV-340, Lutron). The irradiation times were set at 1, 3 and 12 h and ten disks were treated at each UV dose. To treat the resin-TiO_2 disks with UV irradiation in water, the disks were placed in a well of a 6-well plate containing 10 mL of deionized water and covered with a transparent lid. The disks were irradiated with a UV-A diode with an intensity of 10 mW/cm^2 for 3, 5, 6.5, 8 and 16 h and ten disks were treated at each UV dose.

Resin disks without TiO_2 were subjected to a 16 h dose of UV-A radiation in water at the same intensity given to the resin-TiO_2 disks. After the UV treatment, the sample disks were rinsed thoroughly with deionized water and air-dried. All further tests and characterization were performed at least 12 h after the UV treatment.

Surface Characterization

Surface roughness of the resin-TiO_2 disks was analysed with the aid of a surface profiler (WYKO NT1100, Veeco Instruments Inc.). Hydrophobicity of the samples was evaluated through water contact angle measurements. Student's *t*-test was performed to investigate the significance of differences among groups of samples. Surface morphology of samples was analysed with Scanning Electron Microscopy (SEM). Before SEM observation, the disks were sputter coated with gold/palladium (Polaron SC7640, Thermo VG Scientific, England). SEM images were recorded with a LEO 1550 SEM (Zeiss, Oberkochen, Germany) using the in-lens detector and 10 kV acceleration voltage.

Bioactivity tests

Bioactivity of the resin-TiO_2 disks was evaluated according to the amount of hydroxyapatite growth on the sample disk surface after soaking in DPBS (with $CaCl_2$ and $MgCl_2$; Sigma, Steinheim, Germany). One group of resin disks with 16 h UV irradiation (resin disks) and six groups of resin-TiO_2 disks with different UV treatments were tested, including control disks without UV treatment, disks that received 3 and 12 h UV irradiation in air, and disks that received 3, 8 and 16 h UV irradiation while submerged in water. Each disk was soaked in 50 mL sterile DPBS at 37 °C for 7 days, a method that has previously been used to validate *in vitro* bioactivity [6]. After the soaking procedure, each disk was removed from the DPBS, rinsed thoroughly with deionized water and air-dried. The disks were sputter coated with gold/palladium and SEM images were recorded with LEO 1550 SEM using the in-lens detector and 10 kV acceleration voltage. The elemental composition of the observed mineral layer on the surface was analysed with Energy Dispersive Spectrometry (EDS) performed with instrumentation combined in the SEM. The crystalline phase of the deposition layer on the surface was analysed with X-ray diffraction (XRD, Siemens, D5000 X-ray Diffractometer).

Cytotoxicity and cell adhesion tests

Samples for cytotoxicity and cell adhesion tests included UV-irradiated resin disks, resin-TiO2 disks without UV irradiation (Control disks) and UV-irradiated resin-TiO2 disks (3 and 12 h UV in air, 3, 8 and 16 h UV in water), all soaked in DPBS for 7 d.

Two cell lines, human dermal fibroblasts (hDF) and osteoblast-like human osteosarcoma cell line (MG63) were chosen for cytotoxicity tests. The bone-related cell line, MG63, was chosen for cell adhesion tests. All cell lines were cultured in complete growth medium (CGM) containing Dulbecco's modified eagle medium (DMEM/F12) with 10% fetal bovine serum (FBS), penicillin (100 U/ml) and streptomycin (100 µg/ml) in an incubator at 37 °C and 5% CO_2 in a humidified atmosphere. The cells were harvested with trypsin-EDTA and cell density was determined with hemocytometer. All reagents for cell culturing were purchased from Thermo Scientific™ HyClone™.

Cytotoxicity tests were performed according to ISO 10993-5 procedures. Each sample disk was extracted in CGM (ratio of 0.2 g material to 1 ml CGM) in a 24-well tissue culture plate for 24 h at 37 °C and 5% CO_2. The extract medium was used to culture hDF and MG63 cells in a density of 105 cells/ml in a 48 well tissue culture plate for 24 h at 37 °C and 5% CO_2. The CGM extract of the cell culture wells without materials was used as negative control and cell culture with addition of 0.1% Triton X-100 in CGM was used as positive control. Tests were run in triplicate. The viability of hDF was evaluated with the AlamarBlue Assay® (Life Technology) according to the supplied instructions. Cell viability, indicated by

fluorescent intensity, was measured with a plate reader (Tecan Infinite® M200 Pro) with excitation at 560 nm and emission at 590 nm.

For cell adhesion tests, sample disks were placed in 24-well cell culture plates. Each well with a sample disk was seeded with 500 µl of MG63 cell suspension of 105 cells/ml. Cells were cultured for 24 h in an incubator at 37 °C and 5% CO_2 in a humidified atmosphere. To prepare the sample disks for SEM observation, each disk was washed gently with PBS and fixed with 2.5% (v/v) glutaraldehyde in PBS. The sample disks were then dehydrated with a series of ethanol solutions (30%, 50%, 70%, 80%, 90% and twice in 100%) and subsequently a series of ethanol / hexamethyldisilazane (HMDS) solutions (HMDS: ethanol 1:2, HMDS: ethanol 2:1 and pure HMDS). The disks were subsequently sputter coated with gold/palladium and SEM images were recorded with LEO 1550 SEM using secondary electron detector and 5 kV acceleration voltage. Cell density and morphology were investigated.

Bacterial adhesion testing

Gram-positive *Staphylococcus epidermidis* (CCUG 18000A) was chosen for bacterial adhesion testing because it is a skin flora species and a common cause of implant or biomedical device related infections [19].

S.epidermidis was inoculated in Brain Heart Infusion (BHI) broth and incubated at 37 °C until the bacterial growth reached late log phase. Bacteria were then collected by centrifugation and re-suspended in sterile phosphate buffered saline (PBS) to attain a bacterial concentration corresponding to an optical density measurement of OD_{660} = 0.1. Ten milliliters of this bacterial suspension was added to a well in 6-well plate and sample resin-TiO_2 disks were placed symmetrically on the bottom of the well. A rubber ring the same thickness as the disks was situated along the outside wall in the well to keep the disks from contact with the walls of the well, which otherwise resulted in uneven growth of bacteria due to non-uniform fluid flow during incubation. The well plate was fixed to an orbital shaking incubator (Talboys, Troemner, USA) set at 37 °C and the bacteria were incubated for 90 min: first without shaking for 30 min to let bacteria initially settle and adhere to the disk surface, then with 100 rpm orbital shaking for 60 min to create fluid shear forces at the disk surface. Three samples disks from each UV treatment condition were tested.

After the adhesion incubation, the resin-TiO_2 disks were removed from the well and gently rinsed serially in 5 wells with sterile PBS to remove loosely adhered bacteria. Each disk was then put upside-down in a well of 48-well plate with 500 µL sterile PBS and the plate was placed in an ultrasonic bath for 1 min to detach the remaining adherent bacteria from the surface (this procedure was previously tested and shown to have a detaching efficiency > 99.9%). The amount of viable bacteria removed from each disk by the ultrasonic bath was quantified using a metabolic assay incorporating resazurin. Specifically, 100 µL of this bacterial suspension was transferred to a well with 900 µL BHI broth with resazurin (1.25 µg/mL) in 48-well plate. A calibration series of *S. epidermidis* suspension with known bacterial concentration was also included to provide a standard curve. The plate was incubated at 37 °C for 4 h and the production of resorufin due to bacterial metabolic activity (hence corresponding to the amount of viable bacteria) was quantified with a fluorescent multiplate reader (Tecan Infinite® M200 Pro Excitation at 530 nm, Emission at 590 nm). The number of viable bacteria in each test well was determined by correlation with the *S. epidermidis* standard curve.

Results

Surface Characterization

Surface roughness The change in surface roughness of the resin-TiO_2 disks due to the UV treatment is shown in Fig. 1. The roughness Ra (arithmetic average) of the control disks is 124.88 nm. For the sample disks irradiated with UV under ambient conditions (UV, disks in air), 3 h of UV irradiation did not change the surface roughness significantly while 12 h of UV irradiation caused an increase in surface roughness by a factor of four. Conversely, UV irradiation of disks immersed in water led to a decrease in surface roughness with increased UV irradiation. After UV irradiation for 3, 8 and 16 h, the surface roughness decreased to 65 %, 55 % and 40 %, respectively, of the roughness of the control disks. The significance of difference between the control group and all UV treated groups except 3 h in air was confirmed with student's *t*-test ($p < 0.05$).

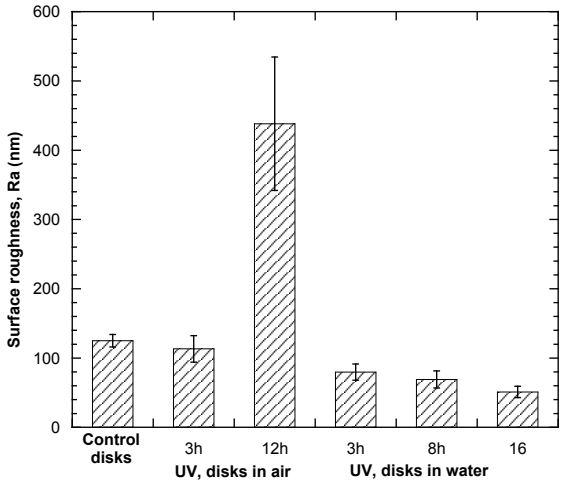

Figure 1. Surface roughness (Ra) change of resin-TiO_2 nanocomposite disks after irradiation with different doses of UV in ambient or water environments. Error bars represent the standard deviation and are based on 5 measurements on different disks.

Hydrophobicity The change in hydrophobicity of the resin-TiO_2 nanocomposite surface due to UV irradiation is shown in Fig. 2. For both sample groups, UV irradiation resulted in a decreased water contact angle on the resin-TiO_2 surface, which indicates that a more hydrophilic surface was produced. The contact angle was also observed to decrease with increasing UV dose, and occurred at a faster rate on the disks irradiated under ambient conditions compared to the disks submerged in water. For example, the disks irradiated for 3 h in air reduced the contact angle to 41.0° while a similar reduction in contact angle for submerged disks (73.1° to 42.3°) required 16 h of UV irradiation. The differences between the control group and the UV treated groups were confirmed to be significant using to student's *t*-test ($p < 0.05$).

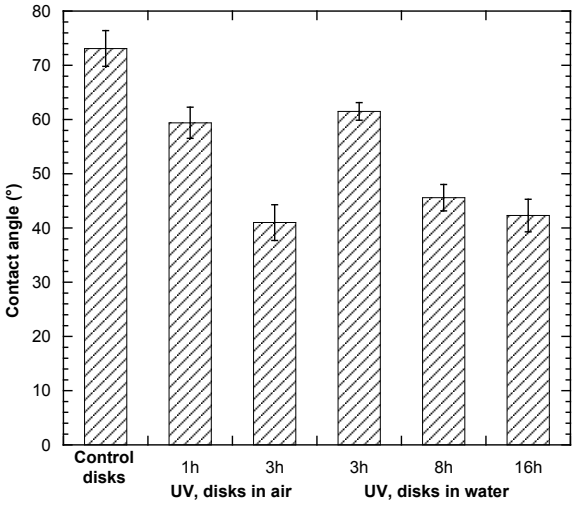

Figure 2. Water contact angle (CA) of resin-TiO_2 nanocomposite surface after UV irradiation in ambient or water environments. Error bars represent the standard deviation and are based on 5 measurements on different disks.

Surface morphology The change in surface morphology of the resin-TiO_2 disks due to the UV irradiation is shown in Fig. 3. Fig. 3-a displays the surface of a control disk, which appears to have a continuous and relatively smooth resin layer covering underlying aggregates of TiO_2 nanoparticles. UV irradiation under ambient conditions results in the creation of holes in the surface of the disk, which is likely due to decomposition of the organic resin matrix through the photocatalysis of TiO_2 (Figs. 3-b and c). However, for samples submerged in water during treatment (Figs.3-d, e and f), UV irradiation did not result in as large of changes in surface morphology as with disks irradiated under ambient conditions. The disk irradiated with 3 h of UV while submerged in water (Fig. 3-d) did not show significant changes in the surface morphology, while 8 h of UV irradiation (Fig. 3-e) resulted in the formation of small holes on the surface. After 16 h of UV irradiation in water (Fig. 3-f), the size of these holes is larger and the encased aggregates of TiO_2 are much less visible.

Bioactivity

Sample disks were observed with SEM after immersion in DPBS for 7 days. Fig.4 shows the growth of a hydroxyapatite layer on the surface of the resin-TiO_2 disks previously treated with different doses of UV irradiation in ambient or water environments, as well as a control disk that did not receive UV treatment. The control disk (Fig.4-a) and the disk treated with 3 h UV irradiation in air (Fig.4-b) showed no hydroxyapatite growth. When UV treatment time was increased to 12 h, subsequent soaking in DPBS resulted in a limited coverage of hydroxyapatite on the disk surface consisting of smaller, isolated crystals. On the other hand, UV treatment of disks submerged in water resulted in better hydroxyapatite growth when subsequently soaked in DPBS. UV irradiation for 3 and 8 h (Fig. 4-d and e) showed a similar density of hydroxyapatite crystals on the surface of resin-TiO_2 nanocomposite where the size of the crystals on the 8 h sample was larger and therefore provided a better coverage of the disk surface. Resin-TiO_2 disks treated with 16 h UV irradiation (disks in water) showed total coverage of the surface with hydroxyapatite after soaking in DPBS for 7 days (Fig. 4-f).

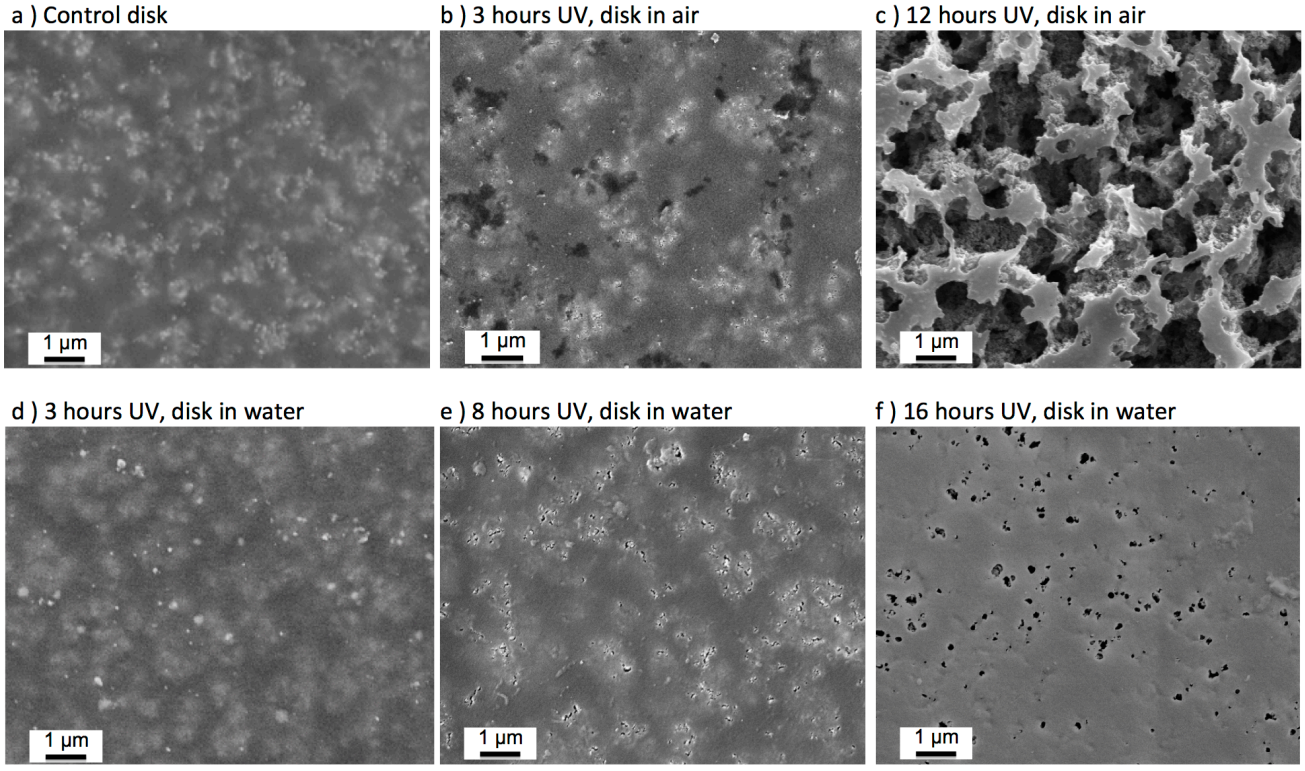

Figure 3. SEM images of a resin-TiO_2 control disk (panel a) and disks treated with different doses of UV irradiation under ambient (panels b, c) or while submerged under water (panels d – f).

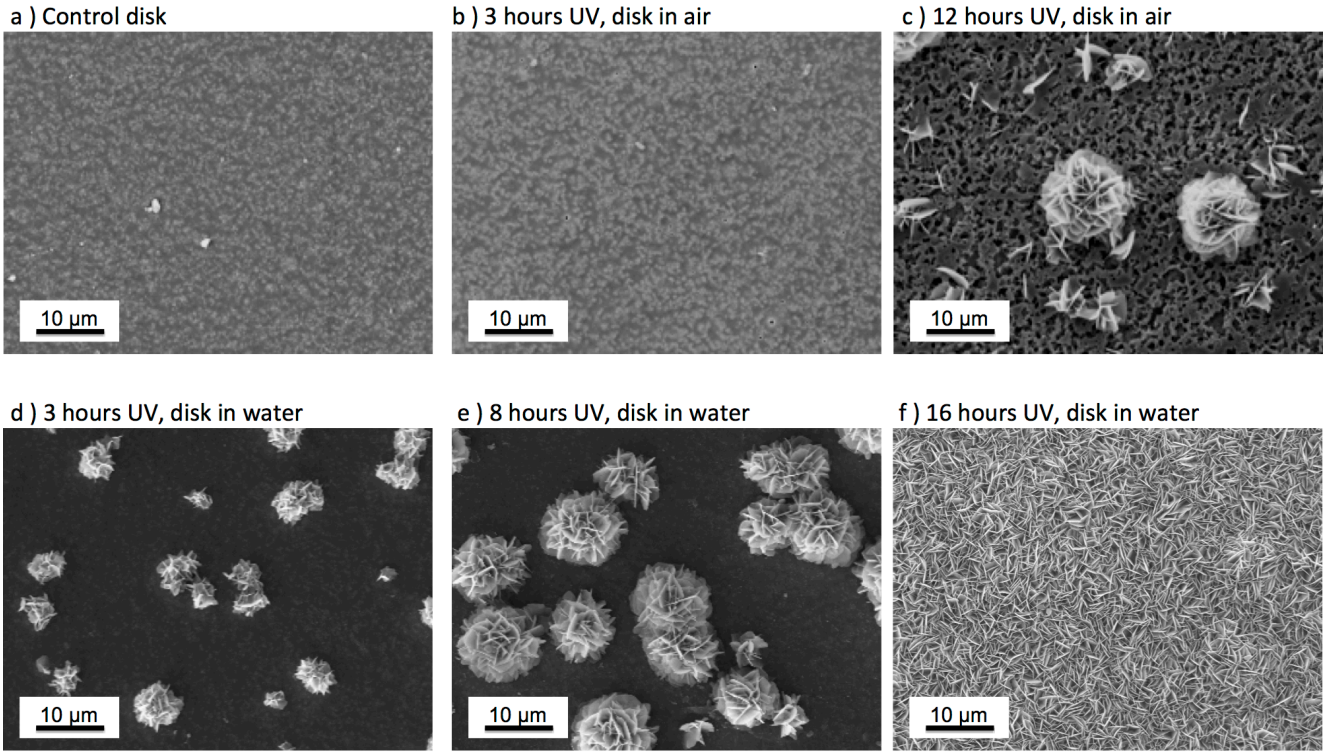

Figure 4. SEM images of resin-TiO_2 disks after 7 d soaking in DPBS. Panel a shows a control disk, panels b and c show disks previously treated with UV under ambient conditions, and panels d – f show disks previously treated with UV while submerged in water.

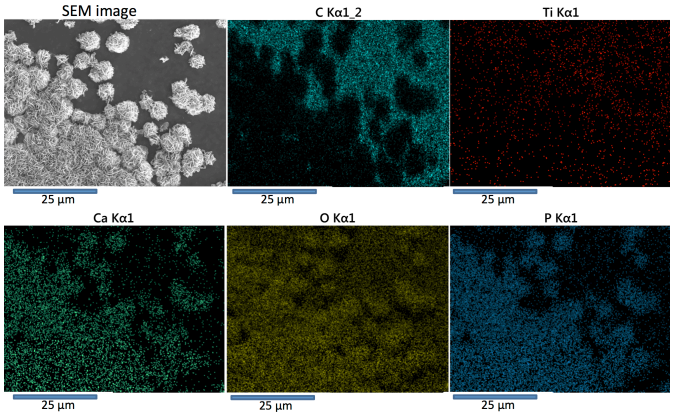

Figure 5. EDS analysis of hydroxyapatite crystal growth on the surface of resin-TiO_2 disks treated with 8 h UV irradiation while submerged in water prior to soaking in DPBS for 7 d. First panel shows the original SEM image while other panels provide coloured overlay mapping of specified elements

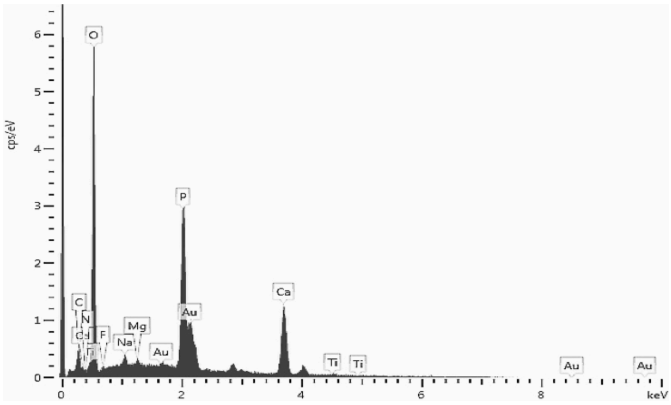

Figure 6. EDS point analysis of the hydroxyapatite layer on the surface of a resin-TiO_2 disk treated with 8 h UV irradiation while submerged in water, then soaked in DPBS for 7 d.

Fig. 5 and 6 show EDS analysis of a sample treated with 8 h of UV irradiation while submerged in water. EDS analysis was performed to investigate the composition of the mineral layer formed on the surface of resin-TiO_2 disks after soaking in DPBS for 7 d. Fig.5 shows the distribution of the key elements over an area on the surface that is partially coated while Fig.6 shows the EDS spectrum of a point analysis on the coated portion of the disk surface. The results show that the coating contains Ca, P and O, providing support for assumption that the coating is hydroxyapatite, a thermodynamically favourable crystalline structure of calcium phosphate in the wet environment [20]. Fig.7 shows an XRD analysis of a sample treated with 16 h of UV irradiation while submerged in water, then soaked in DPBS for 7 days. Distinct hydroxyapatite peaks indicate the crystalline structure of the deposited mineral layer. Furthermore, titania anatase and rutile peaks can also be observed, which are attributed to the P25 TiO_2 nanoparticles encased in the resin matrix.

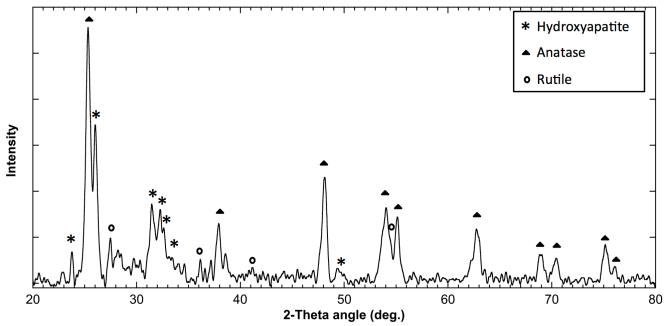

Figure 7. XRD analysis of the hydroxyapatite layer on the surface of a resin-TiO_2 disk treated with 16 h of UV irradiation while submerged in water, then soaked in DPBS for 7 d. Diffraction peaks pertaining to hydroxyapatite, anatase and rutile are indicated.

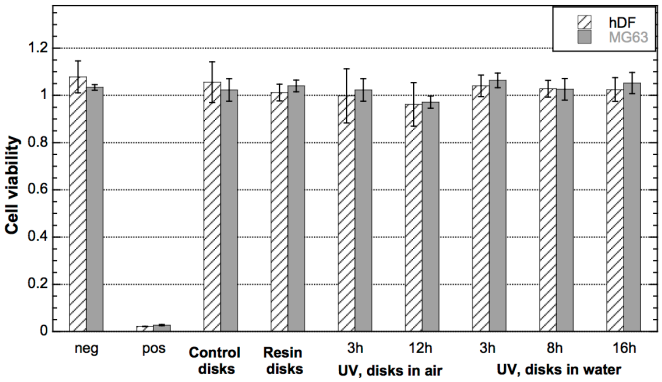

Figure 8. Cell viability of hDF and MG63 after culture in CGM extract of sample disks. Negative control (neg) is the CGM extract in the culture plate and positive control (pos) is the negative control cell culture with addition of 0.1% Triton X-100. Error bars represent the standard deviation, and are based on triplicate tests.

Cytotoxicity and cell adhesion tests

Cytotoxicity and cell adhesion tests were performed to evaluate the potential of UV-irradiated resin-TiO2 nanocomposites in biomedical applications. Eluting tests allow possible toxic substances to diffuse into the CGM from the samples, which will subsequently affect the viability of the cultured cells. Fig. 8 shows the results of the cytotoxicity tests of sample disks against hDF and MG63 cell lines. All samples, including 16 h UV-irradiated resin disks and resin-TiO2 disks, with or without UV irradiation, were found to be nontoxic. In the cell adhesion tests with osteoblast-like MG63 cells (Fig. 9), the sample disks with better hydroxyapatite coverage showed better cell adhesion. After the hydroxyapatite deposition in DPBS, the resin-TiO2 disks that had received 3 and 12 h UV irradiation in air (Fig. 9- b and c) showed limited numbers of cells adhering to the surface. Compared to the UV in air group, the disks that received 3, 8 and 16 hours UV irradiation in water (Fig. 9-d, e and f) showed better hydroxyapatite growth, which appears to be conducive to cell adhesion. Longer UV irradiation led to better coverage of hydroxyapatite and therefore higher cell density in the cell adhesion tests. Resin-TiO_2 without UV irradiation (Control group) did not show hydroxyapatite growth or cell adhesion (Fig. 9-a). The pure resin disk with 16 h UV irradiation followed DPBS soaking also did not lead to hydroxyapatite growth or cell adhesion (Fig. 9-g). Hence, to induce bioactivity of the organic resin material, both TiO_2 and UV irradiation are necessary.

Bacterial adhesion tests

Bacterial adhesion tests were performed to investigate the influence of UV treatment on the tendency for bacteria to subsequently adhere to the surface of the sample disks. Fig. 10 shows the number of *S. epidermidis* that adhered on the sample disks after 1.5 h incubation with bacterial suspension. Compared to the control disks, the disks that received UV irradiation while submerged in water showed decreased bacterial adhesion with increased UV irradiation dose. The disks with 16 h UV irradiation showed 27% less bacterial adhesion compared to the control disks. The disks that received UV irradiation under ambient conditions showed an even greater decrease in bacterial adhesion with a relatively short time of UV irradiation. UV irradiation for 1 or 3 h led to an approximately 43% decrease in bacterial adhesion. However, 12 h of UV irradiation under ambient conditions, showed increased bacterial adhesion on the surface compared to the control disk.

Discussion

The resin-TiO_2 nanocomposite in this study has previously been shown to possess excellent antibacterial properties during UV illumination due to photocatalysis of the encased TiO_2 nanoparticles [16]. In the present paper we investigated the changes in the properties of resin-TiO_2 nanocomposite surface resulting from relatively long term UV irradiation.

From Fig.10 it can be observed that the UV treatment affected bacterial adhesion, which may be attributed to changes in hydrophilicity and surface roughness of the disks. UV irradiation of the resin-TiO_2 disks under both ambient conditions (1-3 h) and while submerged in water (up to 16 h) resulted in decreased hydrophobicity with increased irradiation. In the case of irradiation under ambient conditions, bacterial adhesion was reduced by 43% with only 1 h of irradiation, while 16 h of irradiation of the disks submerged in water resulted in a surface to which 27% less bacteria adhered compared to the control disk. Previous studies have also shown a lower adherence to more hydrophilic surfaces for *S. epidermidis* bacteria [21]. However, a longer time of UV irradiation under ambient condition (12 h) resulted in an increased bacterial adherence, which likely can be attributed to the dramatic increase in surface roughness that can be also observed in Fig. 3-c. Here the photocatalysis of TiO_2 appears to have caused significant decomposition of the organic materials in the composite, resulting in the surface roughness increasing from 124.9 nm to 438.3 nm. It has been shown that surface roughness has a significant effect on *S. epidermidis* attachment when the roughness is higher than 200 nm [22].

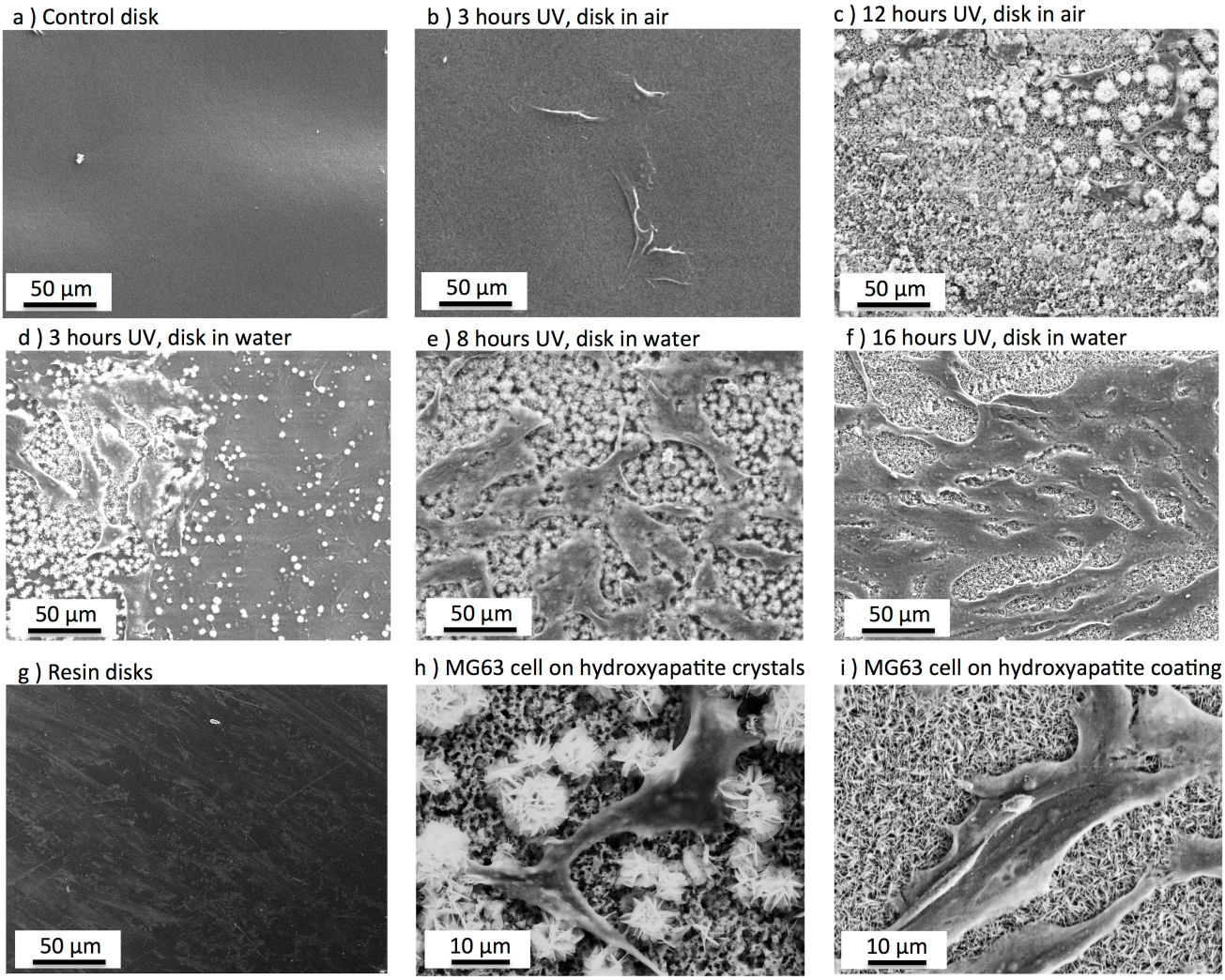

Figure 9. Adhesion of osteoblast-like cells, MG63, on UV treated and subsequently DPBS soaked sample disks (b-f). Samples disks without UV irradiation (a) and without TiO_2 addition (g) served as control groups. The adhered cells on isolated hydroxyapatite crystals (h) and full hydroxyapatite coating (i) are shown in higher magnification.

Perhaps an even more important benefit of the UV treatment is its ability to impart bioactivity to the otherwise non-bioactive resin-TiO_2 surface. Bioactivity of disks treated with varying doses of UV irradiation in air or water environment was evaluated by the amount of growth of hydroxyapatite on the surface after immersion in DPBS for 7 days and subsequently the cell adhesion of osteoblast-like cells. It was found that resin-TiO_2 disks that received UV irradiation while submerged in water produced a more bioactive surface than disks irradiated with UV in ambient conditions. A UV treatment time of 12 h under ambient conditions was required to induce the limited formation of hydroxyapatite crystals displayed in Fig. 4-c while hydroxyapatite crystal formation was observed after only 3 h of UV irradiation on disks submerged in water. Disk surfaces were fully covered with a hydroxyapatite layer on disk surfaces that received a 16 h UV treatment while submerged in water. This degree of hydroxyapatite deposition is much greater than that achieved in other attempts to develop bioactivity on organic materials with aid of TiO_2, which has been shown to take 21-28 days of soaking SBF to achieve similar hydroxyapatite coverage [14, 15] or has resulted in a lower density of hydroxyapatite nucleation [16]. From the cell adhesion

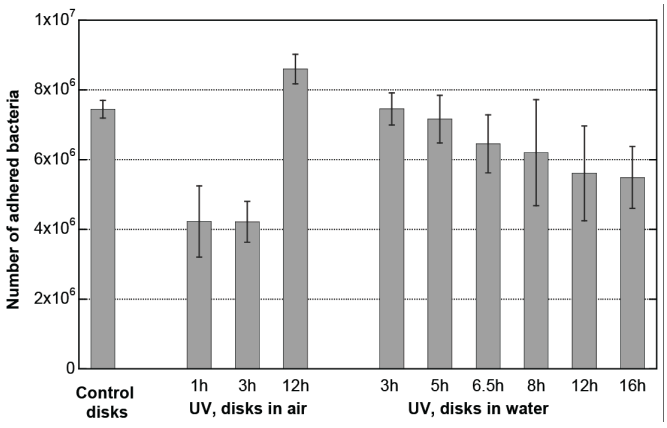

Figure 10. Bacterial adhesion on resin-TiO_2 disks that received varying UV irradiation doses in water or air environments, compared to control disks without UV irradiation. Error bars represent standard deviation based on three measurements.

tests, we could prove that the hydroxyapatite layer is more favoured for cell adhesion than the resin-TiO_2 surface. Better hydroxyapatite coverage of the surface led to a higher density of adhered cells.

There are a number of possible factors that may explain the bioactivity induced by photocatalysis of TiO_2. One factor is the potential exposure of TiO_2 nanoparticles after photocatalytic reaction. Initially the nanoparticles appear to be encased in the resin matrix, as can be seen in the SEM image of the control disk, Fig. 3-a. This organic resin surrounding the TiO_2 nanoparticles can be oxidized by reactive oxygen species (ROS) produced by the photocatalytic reaction, and will consequently decompose into H_2O and CO_2, leaving TiO_2 nanoparticles exposed on the surface. Crystalline TiO_2 is known to be *in vitro* bioactive and therefore the exposed TiO_2 nanoparticles, which consist of both anatase and rutile crystalline phases, would act as nucleus for hydroxyapatite formation. We have previously shown that exposing the nanoparticles in a similar dental adhesive-TiO_2 composite via chemical etching enhances bioactivity [16]. However, the resin-TiO_2 disk with highest degree of bioactivity (Fig. 4-f) does not appear to have a high degree of nanoparticles exposure and therefore other factors likely also play a role in inducing bioactivity.

Another potential factor is the molecular and surface charge modifications produced by the photocatalytic reaction products (ROS). Materials with negatively charged surfaces and abundant hydroxyl groups (–OH), like TiO_2, are likely to induce apatite formation [12]. The carboxylate group ($–COO^-$) is critical for hydroxyapatite formation on polymers because it serves as the initial attractor for Ca^{2+} ions [23]. The primary radicals produced in photocatalytic reaction are the hydroxyl radical (•OH) and the superoxide radical ($O_2^{\bullet -}$). Radicals with high reactivity (e.g., •OH and $O_2^{\bullet -}$) may chemically modify the surface of the resin polymer or TiO_2 nanoparticles. Data on degree of polymerization in HEMA/BisGMA polymer systems like the one used in this study suggest incomplete polymerization (about 88%) [18], and therefore the existence of carbon double bonds of the methacrylate monomer, especially the cross-linker BisGMA, is highly probable. Such an unsaturated carbon double bond would be a sensitive target for oxidation by ROS [24] and thus may be modified by functional groups, like hydroxyl groups (–OH) or carboxylate groups ($–COO^-$). Additionally, the aqueous environment makes the diffusion of radicals possible (as much as 1 μm from the catalyst) [25], so they may have the opportunity to react with sensitive targets on the surface rather than resulting in just decomposing the organic material adjacent to the TiO_2 nanoparticle. This could help explain the lower amount of surface morphology change and better bioactivity of the disks submerged in water during UV irradiation compared to those that received UV irradiation under ambient conditions. A third factor that could help explain the observed degree of bioactivity is the increase in hydrophilicity of the surface as a result of UV irradiation. The decrease in contact angle (i.e. increase in hydrophilicity) with increasing UV treatment for the disks submerged in water correlates with an increase in bioactivity, as can be seen from Fig. 2 and 4. Morozowich et al. [23] have also found that hydroxyapatite growth is favoured on hydrophilic polymers versus hydrophobic polymers. However, similar contact angles were measured on samples that were irradiated under ambient conditions for 1 and 3 h, but these samples did not induce hydroxyapatite formation on their surfaces. Certainly this factor cannot solely explain the induced bioactivity.

This study shows great potential for improvement of existing biomaterials and development of new ones. First, addition of TiO_2 nanoparticles to resin based materials, which are clinically used as dental restoration materials, could hinder formation of secondary caries through the antibacterial action of the photocatalytic TiO_2 under on-demand UV irradiation [16]. Furthermore, a decrease in the tendency for bacterial adhesion on resin-TiO_2 materials following the application of UV light would lower the risk of secondary caries. Second, the photocatalytic reaction may provide a new strategy for endowing organic materials with bioactivity, i.e. deposition of a hydroxyapatite layer on the surface of the polymer materials. This would be beneficial for bone contacting materials due to better cell recognition and adhesion, for example, acrylic bone cement [26]. Third, biomimetic hydroxyapatite coating provides possibilities for loading and releasing drugs or other active agents [2].

Conclusion

In this paper, we present a new strategy to develop bioactivity on a non-bioactive surface of a resin-TiO_2 nanocomposite through photocatalysis of TiO_2. Both reduced bacterial adhesion and improved bioactivity are desirable properties of an implant material, and we have demonstrated that UV pretreatment of the resin-TiO_2 disks, particularly while submerged in water, can achieve both these properties. Combining bioactivity, decreased bacterial adhesion and the highly efficient disinfection ability under UV irradiation suggest that polymer-TiO_2 nanocomposite materials could be interesting candidates for future biomaterials applications.

Acknowledgements

We greatly acknowledge The Carl Trygger Foundation, The Göran Gustafsson Foundation, The Swedish Research Council, Vinnova and The Swedish Foundation For Strategic Research for financially supporting this work.

Notes and references

[a] Nanotechnology and Functional Materials, The Ångström Laboratory, Uppsala University, Uppsala, Sweden
[b] Applied Materials Science, The Ångström Laboratory, Uppsala University, Uppsala, Sweden
* Corresponding authors: Tel: +46700782780; Email address: caiyanling@hotmail.com (Y.L. Cai); Tel: +46184717944; Email address: ken.welch@angstrom.uu.se (K.Welch).

1 L. L. Hench, R. J. Splinter, W. C. Allen and T. K. Greenlee, *Journal of Biomedical Materials Research Symposium*, 1972, **2**, 117-141.
2 J. Forsgren, U. Brohede, S. Piskounova, A. Mihranyan, S. Larsson, M. Strømme and H. Engqvist, *Journal of Biomaterials and Nanobiotechnology*, 2011, **2**, 149-154; S. Piskounova, J. Forsgren, U. Brohede, H. Engqvist and M. Strømme, *Journal of Biomedical Materials Research, Part B*, 2009, **91B**, 780-787; J. Forsgren, U. Brohede, M. Strømme and H. Engqvist, *Biotechnology Letters*, 2011, **33**, 1265-1268.
3 U. Brohede, J. Forsgren, S. Roos, A. Mihranyan, H. Engqvist and M. Strømme, *Journal of Materials Science: Materials in Medicine*, 2009, **20**, 1859-1867.
4 T. Kokubo, *Biomaterials*, 1991, **12**, 155-163.
5 T. Kokubo, *Thermochimica Acta*, 1996, **280**, 479-490.
6 J. Forsgren, F. Svahn, T. Jarmar and H. Engqvist, *Acta Biomaterialia*, 2007, **3**, 980-984.
7 A. Mihranyan, J. Forsgren, M. Strømme and H. Engqvist, *Langmuir*, 2009, **25**, 1292-1295;U. Brohede, S. X. Zhao, F. Lindberg, A. Mihranyan, J. Forsgren, M. Strømme and H. Engqvist, *Applied Surface Science*, 2009, **255**, 7723-7728; M. Lilja, A. Genvad, M. Åstrand, M. Strømme and H. Enqvist, *Journal of Materials Science: Materials in Medicine*, 2011, **22**, 2727-2734; I. P. Grigal, A. M. Markeev, S. A. Gudkova, A. G. Chernikova, A. S. Mityaev and A. P. Alekhin, *Applied Surface Science*, 2012, **258**, 3415-3419.

8 A. Sugino, K. Tsuru, S. Hayakawa, K. Kikuta, G. Kawachi, A. Osaka and C. Ohtsuki, *Journal of the Ceramic Society of Japan*, 2009, **117**, 515-520.
9 J. Forsgren, F. Svahn, T. Jarmar and H. Engqvist, *Journal of Applied Biomaterials & Biomechanics*, 2007, **5**, 23-27; F. Lindberg, J. Heinrichs, F. Ericson, P. Thomsen and H. Engqvist, *Biomaterials*, 2008, **29**, 3317-3323.
10 T. Kokubo and H. Takadama, *Biomaterials*, 2006, **27**, 2907-2915.
11 M. Svetina, L. C. Ciacchi, O. Sbaizero, S. Meriani and A. De Vita, *Acta Materialia*, 2001, **49**, 2169-2177.
12 P. J. Li, C. Ohtsuki, T. Kokubo, K. Nakanishi, N. Soga and K. Degroot, *Journal of Biomedical Materials Research*, 1994, **28**, 7-15.
13 H. M. Kim, H. Kaneko, M. Kawashita, T. Kokubo and T. Nakamura (2004) *Mechanism of apatite formation on anodically oxidized titanium metal in simulated body fluid*. 741-744. Zurich-Uetikon: Trans Tech Publications Ltd; C. Lindahl, P. Borchardt, J. Lausmaa, W. Xia and H. Engqvist, *Journal of Materials Science: Materials in Medicine*, 2010, **21**, 2743-2749.
14 A. R. Boccaccini, L. C. Gerhardt, S. Rebeling and J. J. Blaker, *Composites Part a, Applied Science and Manufacturing*, 2005, **36**, 721-727.
15 L. C. Gerhardt, G. M. R. Jell and A. R. Boccaccini, *Journal of Materials Science: Materials in Medicine*, 2007, **18**, 1287-1298.
16 K. Welch, Y. Cai, H. Engqvist and M. Strømme, *Dental Materials*, 2010, **26**, 491-499.
17 M. Lilja, J. Forsgren, K. Welch, M. Åstrand, H. Engqvist and M. Strømme, *Biotechnology Letters*, 2012, **34**, 2299-2305;M. Lilja, K. Welch, M. Åstrand, H. Engqvist and M. Strømme, *Journal of Biomedical Materials Research, Part B*, 2012, **100B**, 1078-1085. Y. Cai, M. Strømme, Å. Melhus, H. Engqvist, and K. Welch, *J. Biomed. Mater. Res. B – Appl. Biomater.* 2014, **102**, 62-67; Y. Cai, M. Strømme, and K. Welch, *3Biotech*, 2014, **4**, 149-157; Y. Cai, M. Strømme, and K. Welch, J. Biomater. Nanobiotech., 2014, **5**, 200-209; Y. Cai, M. Strømme, and K. Welch, *PLoSONE*, 2013, **8**, e75929.
18 J. Park, Q. Ye, E. M. Topp, A. Misra, S. L. Kieweg and P. Spencer, *Journal of Biomedical Materials Research, Part A*, 2010, **93A**, 1245-1251.
19 J. D. Patel, E. Colton, M. Ebert and J. M. Anderson, *Journal of Biomedical Materials Research, Part A*, 2012, **100A**, 2863-2869.
20 T. Kokubo, *Materials Science & Engineering C-Biomimetic and Supramolecular Systems*, 2005, **25**, 97-104; H. M. Kim, T. Himeno, T. Kokubo and T. Nakamura, *Biomaterials*, 2005, **26**, 4366-4373.
21 C. Sousa, P. Teixeira and R. Oliveira, *International Journal of Biomaterials*, 2009, 718017 ; M. J. Giraldez, C. G. Resua, M. Lira, M. Oliveira, B. Magarifios, A. E. Toranzo and E. Yebra-Pimentel, *Optometry and Vision Science*, 2010, **87**, E426-E431; L. Kodjikian, C. Burillon, C. Roques, G. Pellon, J. Freney and F. N. R. Renaud, *Investigative Ophthalmology & Visual Science*, 2003, **44**, 4388-4394; J. H. Sörensen, M. Lilja, T. Sörensen, M. Åstrand, P.Procter, M. Strømme, H. Steckel, *Current Drug Delivery*, 2014, **11**, 501-510
22 H. Y. Tang, T. Cao, X. M. Liang, A. F. Wang, S. O. Salley, J. McAllister and K. Y. S. Ng, *Journal of Biomedical Materials Research, Part A*, 2009, **88A**, 454-463.
23 N. L. Morozowich, J. L. Nichol and H. R. Allcock, *Chemistry of Materials* 2012, **24**, 3500-3509.
24 J. Kiwi and V. Nadtochenko, *Journal of Physical Chemistry B*, 2004, **108**, 17675-17684.
25 Y. Kikuchi, K. Sunada, T. Iyoda, K. Hashimoto and A. Fujishima, *Journal of Photochemistry and Photobiology a-Chemistry*, 1997, **106**, 51-56.
26 G. Lewis, *Journal of Biomedical Materials Research, Part B*, 2008, **84B**, 301-319.

Bioactivity of resin-TiO_2 nanocomposite induced by TiO_2 photocatalysis under UV irradiation

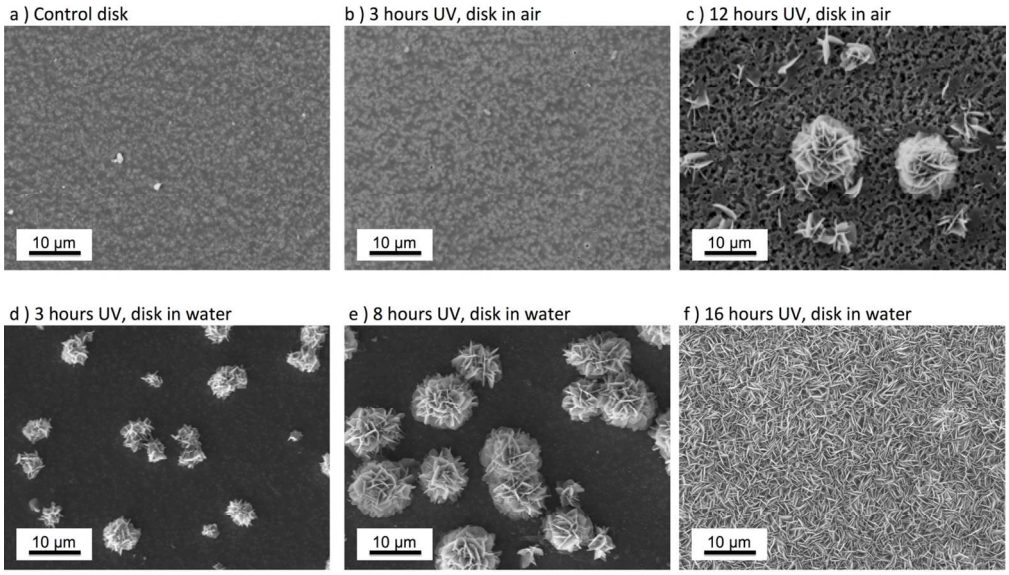

127x95mm (300 x 300 DPI)